Histone Acetylation, Not Stoichiometry, Regulates Linker Histone Binding in *Saccharomyces cerevisiae*

Mackenzie B. D. Lawrence,* Nicolas Coutin,* Jennifer K. Choi,* Benjamin J. E. Martin,* Nicholas A. T. Irwin,* Barry Young,† Christopher Loewen,† and LeAnn J. Howe*,1

*Department of Biochemistry and Molecular Biology and †Department of Cellular and Physiological Sciences, University of British Columbia, Vancouver, British Columbia V6T 1Z3, Canada

ABSTRACT Linker histones play a fundamental role in shaping chromatin structure, but how their interaction with chromatin is regulated is not well understood. In this study, we used a combination of genetic and genomic approaches to explore the regulation of linker histone binding in the yeast, *Saccharomyces cerevisiae*. We found that increased expression of Hho1, the yeast linker histone, resulted in a severe growth defect, despite only subtle changes in chromatin structure. Further, this growth defect was rescued by mutations that increase histone acetylation. Consistent with this, genome-wide analysis of linker histone occupancy revealed an inverse correlation with histone tail acetylation in both yeast and mouse embryonic stem cells. Collectively, these results suggest that histone acetylation negatively regulates linker histone binding in *S. cerevisiae* and other organisms and provide important insight into how chromatin structure is regulated and maintained to both facilitate and repress transcription.

KEYWORDS Hho1; linker histone; histone acetylation; *S. cerevisiae*

In eukaryotes, DNA is packaged into chromatin, a nucleoprotein structure composed of DNA, histones, and nonhistone proteins. The basic repeating unit of chromatin is the nucleosome core particle, which is composed of DNA wrapped 1.7 times around an octamer of core histones H2A, H2B, H3, and H4 (Van Holde 1989; Luger *et al.* 1997). A fifth histone protein, termed the "linker histone," binds the nucleosome dyad, interacting with the DNA entering and exiting the nucleosome (Syed *et al.* 2010; Meyer *et al.* 2011; Zhou *et al.* 2013, 2015; Bednar *et al.* 2017). Because linker histones limit DNA accessibility and promote chromatin compaction, they are thought to be general repressors of transcription (Bustin *et al.* 2005; Happel and Doenecke 2009), and regulating their interaction with chromatin may provide a means to control access of the transcriptional machinery to DNA.

One proposed mechanism for regulating linker histone binding is through alteration of linker histone abundance. *Saccharomyces cerevisiae* expresses one molecule of linker histone for every 4–37 nucleosomes (Freidkin and Katcoff 2001; Downs *et al.* 2003), consistent with the gene-dense nature of this yeast's genome. In contrast, vertebrate cells, which have many gene-poor regions, express ~1 molecule of linker histone for every nucleosome, and transcriptionally inert avian erythrocytes express 1.3 linker histones per nucleosome (Woodcock *et al.* 2006). However, several studies have demonstrated that linker histone occupancy is not uniform across the genome of a given cell type, suggesting that factors in addition to protein abundance regulate linker histone binding. For example, the yeast linker histone, Hho1, cross-links poorly to the first nucleosome relative to the transcription start site (TSS) and is instead enriched in regions with increased nucleosome spacing (Rhee *et al.* 2014; Ocampo *et al.* 2016). Further, transcriptionally active regions tend to be depleted in linker histones in multiple organisms (Schafer *et al.* 2008; Cao *et al.* 2013; Izzo *et al.* 2013; Millan-Arino *et al.* 2014; Ocampo *et al.* 2016). One potential mechanism for regulating linker histone binding is via histone acetylation, which is enriched on active genes. Because linker histones bind to nucleosomes via contacts with DNA as it enters and exits the nucleosome, acetylation, which promotes DNA unwrapping, could disrupt Hho1 binding sites (Neumann *et al.* 2009; Syed *et al.* 2010; Meyer *et al.* 2011; Simon *et al.* 2011; Zhou *et al.* 2013, 2015; Bernier *et al.* 2015; Kim *et al.* 2015; Ikebe *et al.* 2016; Bednar *et al.* 2017). Indeed, others have

doi: https://doi.org/10.1534/genetics.117.1132
Manuscript received December 19, 2016; accepted for publication July 12, 2017; published Early Online July 26, 2017.
Supplemental material is available online at www.genetics.org/lookup/suppl/doi:10.1534/genetics.117.1132/-/DC1.
[1]Corresponding author: Department of Biochemistry and Molecular Biology, University of British Columbia, 2350 Health Sciences Mall, Vancouver, BC V6T 1Z3, Canada. E-mail: ljhowe@mail.ubc.ca

observed increased linker histone mobility in cells treated with histone deacetylase inhibitors (Raghuram *et al.* 2010). Despite this evidence, however, the regulation of linker histone binding by core histone acetylation has not been thoroughly explored.

One of the challenges in unraveling the regulation of linker histone function is that most organisms contain multiple linker histone-encoding genes. For example, 11 different linker histone subtypes have been identified in mammals, including seven somatic and four germ line variants (Happel and Doenecke 2009). An attractive model system for studying linker histone function is therefore *S. cerevisiae*, which expresses its linker histone, termed Hho1, from a single gene. However, one of the limitations of this yeast is that the abundance of Hho1 is much lower than that observed in other eukaryotes. Downs *et al.* (2003) estimated linker histone stoichiometry in yeast to be one molecule for every 4 nucleosomes, while data from Freidkin and Katcoff (2001) suggested it is much lower, at one molecule of Hho1 for every 37 nucleosomes. Two high throughput analyses of protein expression in yeast have estimated that there are 2610 and 6560 molecules of Hho1 per haploid cell, representing ratios of 1:26 and 1:10 for the ~68,000 annotated nucleosomes in yeast (Ghaemmaghami *et al.* 2003; Brogaard *et al.* 2012; Kulak *et al.* 2014). Here we designed a novel scheme to determine linker histone stoichiometry in yeast and investigated the impact of *HHO1* overexpression on chromatin structure. Our data suggest that linker histone stoichiometry in yeast is one molecule of Hho1 for every 19 nucleosomes. Moreover, we show that increasing Hho1 levels results in a severe growth defect, despite only modestly impacting Hho1 occupancy or gross chromatin structure. Hho1 toxicity could be rescued by increased histone acetylation, consistent with the negative correlation between linker histone stoichiometry and histone acetylation in both yeast and mouse embryonic stem cells. Collectively these results suggest that factors in addition to linker histone stoichiometry, including histone acetylation, dictate the impact that linker histones have on chromatin structure.

Materials and Methods

Yeast strains and plasmids

All strains used in this study were isogenic to S288C and are available upon request. Yeast culture and genetic manipulations were carried out using standard protocols. Genomic deletions and epitope-tag integrations were verified by PCR analysis. The strains carrying the histone H3 tail mutants were derived by plasmid shuffle from FY2162 (Duina and Winston 2004). The plasmid pGAL1prHHO1 was generated by cloning the *HHO1* ORF into the *Bam*HI/*Xho*I sites of pGAL1pr (Mumberg *et al.* 1994). The pHHT2prHHO1HA plasmid was created by: (1) swapping the *GAL1* promoter from pGAL1prHHO1 with a fragment containing 535 bp upstream of the *HHT2* gene and (2) adding a triple HA tag and *CYC1* terminator at the carboxyl terminus.

Quantitative immunoblot analysis

Whole cell extracts (Kushnirov 2000) were analyzed by immunoblotting for the HA tag (High Affinity 3F10 clone), Hho1 (Abcam, Cambridge, MA; ab71833) or histone H3 (rabbit polyclonal raised against CKDIKLARRLRGERS) followed by fluorescence detection and quantification using the Licor Odyssey System.

Chromatin immunoprecipitation-quantitative PCR analysis

Chromatin immunoprecipitation-quantitative PCR (ChIP-QPCR) analysis was performed as previously described (Martin *et al.* 2017). Cells were grown in 50 ml of synthetic drop-out media lacking uracil with galactose for 20 hr to an OD_{600} of ~0.8 and lysates were immunoprecipitated with 0.9 μg of α-Hho1 antibody (ab71833, Abcam). QPCR was performed using the primers listed in Supplemental Material, Table S1 in File S1.

Micrococcal nuclease digestion of yeast chromatin

Cells were grown in synthetic drop-out media lacking uracil with dextrose until stationary phase, before being washed two times in synthetic drop-out media lacking uracil with galactose. Cells were then diluted in −uracil galactose media to an OD_{600} of 0.2 and grown for 20 hr at 30°. Following harvest, 25 ODs of cells were resuspended in 400 μl of 1 M sorbitol, 5 mM β-mercaptoethanol, and 10 mg/ml zymolyase, and incubated at 37° for 10 min. Spheroplasts were washed once in 1 M sorbitol and twice in spheroplast digestion buffer (SDB) (1 M sorbitol, 50 mM NaCl, 10 mM Tris pH 8, 5 mM $MgCl_2$, 1 mM $CaCl_2$, 1 mM β-mercaptoethanol, 0.5 mM spermidine, 0.075% NP40) before being resuspended in 450 μl of SDB. Samples were digested with varying concentrations of micrococcal nuclease for 2 min and digestions were stopped by addition of EDTA and SDS to final concentrations of 5 mM and 1%, respectively. Cross-links were reversed by overnight incubation at 65° and DNA was purified by digestion with proteinase K, phenol:chloroform:isoamyl extraction, and ethanol precipitation. Samples were resuspended in 10 mM Tris pH 8, 1 mM EDTA, and treated with RNase A prior to running on a 2% agarose gel. DNA was visualized using syto60 fluorescence detection with the Licor Odyssey System.

Synthetic dosage lethality screen

The synthetic genetic array (SGA) starting strain Y7092 (*MAT*α *can1*Δ::*STE2pr-Sp-his5 lyp1*Δ *his3*Δ*1 leu2*Δ*0 met15*Δ *ura3*Δ*0*) was transformed with pGAL1prHHO1. The resulting query strain was mated to the *MAT***a** deletion mutant array. SGA methodology, previously described for a plasmid-based synthetic dosage resistance screen (Chruscicki *et al.* 2010), was performed in triplicate with the following modifications: (1) medium lacking uracil was used to maintain the plasmid, and (2) hits were scored against strains containing pGAL1prHHO1 grown on dextrose using the Balony program (Young and Loewen 2013).

ChIP-sequencing analysis

ChIP-sequencing (ChIP-seq) was performed as previously described with a few alterations (Maltby *et al.* 2012a,b). Briefly, cells were grown in 1 liter of yeast, peptone, dextrose media to mid-log phase and cross-linked with 1% formaldehyde for 15 min at 30°. The cross-linking reaction was stopped with

125 mM glycine and cells were washed twice with cold PBS. Cells were resuspended in lysis buffer [50 mM HEPES-KOH (pH 7.5), 140 mM NaCl, 1 mM EDTA, 1% Triton X-100, 0.1% sodium deoxycholate], flash frozen in liquid nitrogen, and ground in a coffee grinder with dry ice for 10 × 3 min. Samples were thawed, normalized by protein content, and sonicated (Diagenode Biorupter, high output for 30 × 30 sec on/off) to obtain an average DNA fragment length of 200–400 bp. The lysate was cleared at 10,000 rpm for 10 min, and the supernatant was retained for the whole cell extract. Magnetic Protein-G Dynabeads were added and incubated with the whole cell extract for 1 hr, and then removed. Antibodies were added (15.0 μl of the α-Hho1 antibody, ab71833; Abcam) and incubated with the whole cell extract overnight. Magnetic Protein-G Dynabeads were added and incubated with the sample for 30 min. After reversal of cross-linking and DNA purification, the library construction protocol was performed as described (Maltby *et al.* 2012b). Equimolar amounts of indexed, amplified libraries were pooled, adapter dimers were removed by gel purification, and paired-end 100 nucleotide reads were generated using v3 sequencing reagents on the HiSeq2000 (SBS) platform. Reads were aligned to the Saccer3 genome using the Burrows-Wheeler aligner (Li and Durbin 2010), and plot2DO (https://github.com/rchereji/plot2DO) (Chereji *et al.* 2017), Deeptools (Ramirez *et al.* 2014, 2016), and the Java Genomics Toolkit (http://palpant.us/java-genomics-toolkit/) were used for all subsequent analysis as indicated. Additional data used in this manuscript were sourced from https://www.ncbi.nlm.nih.gov/geo/ including GSE61888 (ChIP-seq of histone post-translational modifications in *S. cerevisiae*), GSE38384 (RNAPII ChIP-seq in *S. cerevisiae*), GSE46134 (ChIP-seq of linker histones in mouse embryonic stem cells), and GSE29218 (ChIP-seq of H3K9ac, H3K27ac, and Pol2 in mouse embryonic stem cells).

Data availability

The ChIP-seq data generated for this study have been deposited in the Gene Expression Omnibus (GEO) database (https://www.ncbi.nlm.nih.gov/geo/), GEO accession no. GSE100591.

Results

Refining linker histone stoichiometry in S. cerevisiae

Most eukaryotic chromatin contains approximately one molecule of linker histone for every nucleosome. In *S. cerevisiae*, linker histone stoichiometry is greatly reduced, but attempts to quantify the ratio of linker histone to nucleosomes have led to conflicting results. Previous studies made use of carboxyl-terminal epitope tags to quantify Hho1 levels but, surprisingly, we found that addition of a carboxyl-terminal HA tag to the endogenous *HHO1* gene reduced Hho1 abundance approximately five-fold (Figure S1, A and B in File S1). One explanation for this effect is the native *HHO1* 3′-UTR, which is replaced when carboxyl-terminal epitope tagging, is required for mRNA stability or protein translation. To circumvent this problem,

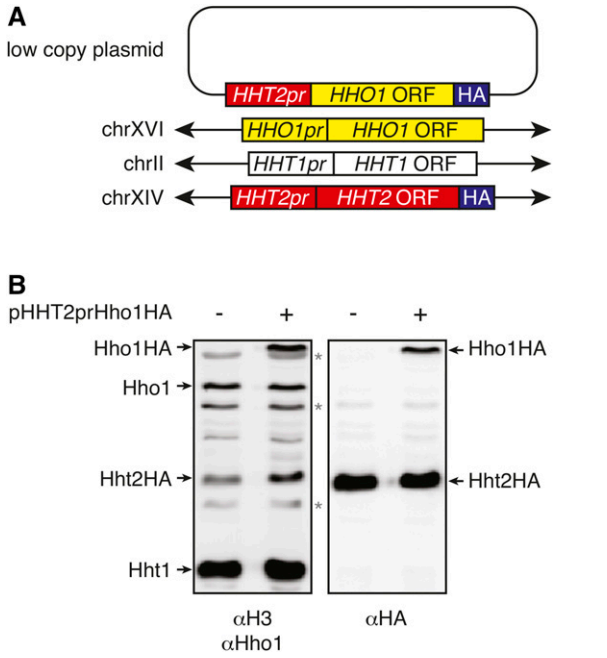

Figure 1 Refining linker histone stoichiometry in *S. cerevisiae*. (A) Schematic representation of the genes encoding histones Hho1 and H3 in an engineered strain of *S. cerevisiae*. Elements from the *HHO1* locus are shown in yellow, the *HHT1* (Histone H Three 1) locus are shown in white and *HHT2* (Histone H Three 2) locus are shown in red. The position of triple HA tags on Hho1 and Hht2 are shown in blue. pr, promoter. (B) Representative immunoblot of whole cell extracts from the strain described in A (+) as well as an isogenic strain lacking the pHHT2prHHO1 plasmid (−). Quantification of Hho1HA with αHA and αHho1 antibodies and H3 with αHA and αH3 antibodies facilitated determination of the relative ratio of Hho1 to histone H3. Bands cross-reacting with the αHho1 antibody are indicated with asterisks.

we sought to quantify the abundance of Hho1 expressed from an unaltered *HHO1* locus relative to a core histone. To this end, we generated a yeast strain expressing two copies of *HHO1* (Figure 1A). The first copy was the endogenous, chromosomal *HHO1* locus, which was unaltered (shown in yellow). The second copy was the *HHO1* ORF (yellow) fused to the histone H3 promoter (*HHT2pr*, shown in red) with a carboxyl-terminal HA tag (blue) on a low-copy plasmid. The yeast strain also included an identical HA tag on one (*HHT2*) of the two copies of the histone H3 gene. By immunoblotting whole cell extracts from this strain for Hho1, HA, and H3, we could directly compare signals generated with the Hho1 and H3 antibodies, using the identical HA tags on Hho1 and H3 (Figure 1B). Using this approach, with three biological replicates, we calculated the linker histone stoichiometry in yeast to be one molecule of linker histone generated from the endogenous *HHO1* locus for every 18.9 ± 1.0 nucleosomes.

Increased linker histone stoichiometry is toxic in S. cerevisiae

Linker histones are thought to negatively regulate transcription and thus the reduced linker histone stoichiometry in *S. cerevisiae* is consistent with the gene-dense nature of

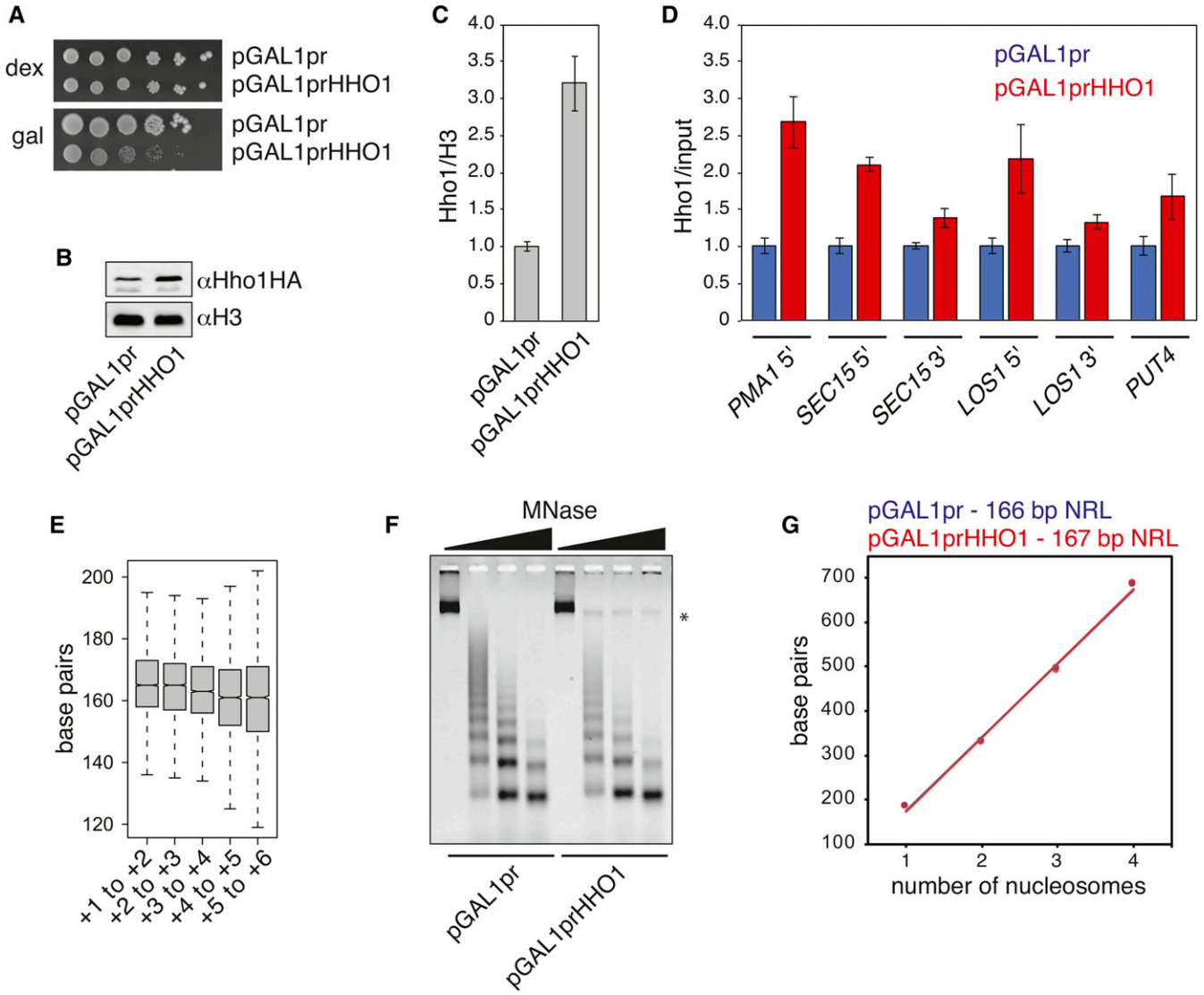

Figure 2 Increased linker histone stoichiometry is toxic in *S. cerevisiae*. (A) Ten-fold serial dilutions of wild-type yeast containing vector alone (pGAL1pr) or expressing *HHO1* from a *GAL1* promoter (pGAL1prHHO1) were plated on uracil drop-out media with dextrose or galactose and grown at 30° for 3 days. (B) Representative immunoblot for Hho1 levels in extracts from cells with vector alone (pGAL1pr) or expressing *HHO1* from a *GAL1* promoter (pGAL1prHHO1) grown for 20 hr in uracil drop-out media with galactose. (C) Quantification of Hho1 levels determined from immunoblot of Hho1 in three biological replicates. Error bars indicate the SE of the mean. (D) ChIP-QPCR for galactose-induced Hho1 at the indicated loci. Cells containing vector alone were set to 1. Error bars indicate SE of the mean of six biological replicates. (E) Box plot of base pair distance between nucleosome positions (Weiner *et al.* 2012) relative to the transcriptional start site. Notches indicate the 95% confidence interval for the median. (F) Chromatin from cells containing vector alone (pGAL1pr) or expressing *HHO1* from a *GAL1* promoter (pGAL1prHHO1) grown for 20 hr in uracil drop-out media with galactose was digested with increasing concentrations of MNase. The DNA was purified and resolved on an agarose gel. (G) Plot of DNA fragment sizes (from F) *vs.* the number of nucleosomes with cells containing vector alone (blue) or expressing *HHO1* from a *GAL1* promoter (red). The indicated nucleosome repeat lengths were determined from the slope of the lines.

the yeast genome. To determine the impact of increased linker histone dosage on growth and chromatin structure of *S. cerevisiae*, we fused the *HHO1* ORF to a *GAL1* promoter (*GAL1pr*) on a low-copy vector and transformed this plasmid into wild-type yeast. Expression of Hho1 from *GAL1pr* resulted in a severe growth defect (Figure 2A), despite increasing total Hho1 abundance only threefold relative to yeast with vector alone (Figure 2, B and C).

To confirm that excess Hho1 is incorporated into chromatin, we performed chromatin immunoprecipitation at multiple loci, including the 5′ end of a highly expressed gene (*PMA1*), the 5′ and 3′ ends of two moderately expressed genes (*LOS1* and *SEC15*), and the middle of *PUT4*, an inactive gene. These results, shown in Figure 2D, demonstrate that *HHO1* overexpression resulted in statistically significant increases (*P*-value for student's *t*-test <0.05) in Hho1 occupancy at all loci tested, with the exception of *PUT4*. Importantly, in no case was the increase in Hho1 occupancy proportional to the over threefold increase in total Hho1 abundance observed in Figure 2C, suggesting that in yeast, linker histone binding is not strictly

dictated by Hho1 levels. Interestingly, the greatest increases in Hho1 binding upon *HHO1* overexpression were observed on the 5′ ends of genes. Previous work has shown that Hho1 is enriched in regions with increased nucleosome spacing (Ocampo *et al.* 2016). To determine whether the differential incorporation of excess Hho1 at 5′ relative to 3′ genic regions was due to increased nucleosome spacing, we calculated the average spacing of nucleosomes relative to all annotated TSSs in yeast (Weiner *et al.* 2015). Figure 2E shows that average nucleosome spacing between the +1 and +2, +2 and +3, and +3 and +4 nucleosomes is 167, 165, and 164 bp, respectively. In contrast, average nucleosome spacing between the +4 and +5, and +5 and +6 nucleosomes is 161 bp, suggesting that these regions are refractory toward Hho1 binding because they lack sufficient linker DNA.

To determine whether *HHO1* overexpression was associated with major changes in chromatin structure, we analyzed the effect of increased Hho1 on the sensitivity of yeast chromatin to micrococcal nuclease (MNase). Figure 2, F and G shows that increased Hho1 levels had little effect on the length of fragments generated by MNase digestion. However, *HHO1* overexpression consistently resulted in loss of fragments larger than four nucleosomes and generation of a high molecular weight, MNase-resistant DNA band (highlighted with an asterisk in Figure 2F), which may suggest that increased levels of Hho1 promotes formation of nuclease-resistant domains at the expense of longer MNase-sensitive, nucleosome arrays. Collectively, these results demonstrate that overexpression of Hho1 results in modest increases in Hho1 occupancy at the 5′ regions of genes, localized changes in chromatin structure, and impaired cell growth.

The specific incorporation of excess Hho1 at the 5′ regions of genes was surprising, considering that previously published work suggests that Hho1 fails to cross-link to the 5′ linker DNA of +1 nucleosomes (Rhee *et al.* 2014). This inconsistency may suggest that, when expressed from its endogenous promoter, Hho1 binding is under some form of regulation. To identify proteins or genetic pathways involved in regulating the interaction of Hho1 with chromatin, we used SGA technology to overexpress Hho1 in the ~4700 nonessential yeast deletion mutants. A major class of genes identified in the screen was those that regulate core histone gene dosage (Table S2) (Kurat *et al.* 2014). Interestingly, decreased growth due to *HHO1* overexpression was observed in mutants predicted to have both decreased and increased histone levels (chi-squared test $P = 0.00263$ for a random distribution). The sensitivity of cells with increased core histone levels to Hho1 overexpression was not surprising, as the combination likely interferes with processes that use DNA as a template. In contrast, the enhanced Hho1 toxicity of cells with reduced core histone levels may be due to increased nucleosome spacing, which creates additional binding sites for Hho1, interfering with DNA access. Indeed, *spt10*Δ, one of the most sensitive strains to *HHO1* overexpression, has been shown to exhibit increased nucleosomes spacing (van Bakel *et al.* 2013).

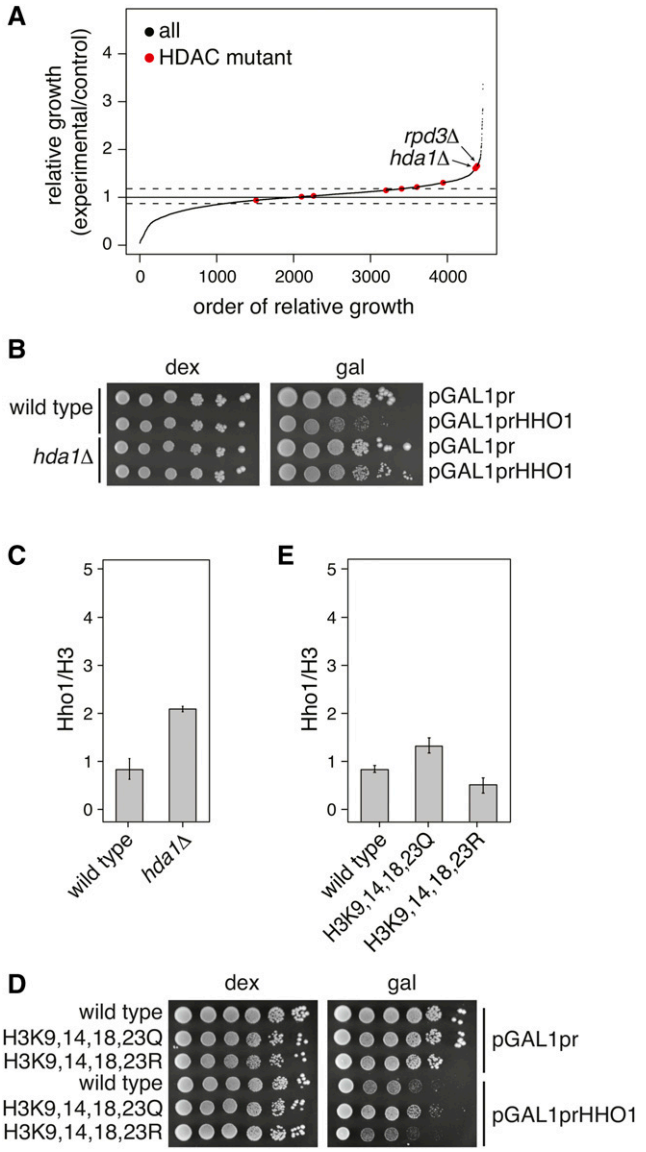

Figure 3 Histone acetylation negatively regulates linker histone binding in *S. cerevisiae*. (A) Relative growth of ~4700 nonessential deletion strains expressing Hho1 from a *GAL1* promoter. Mutants with gene deletions of *RPD3*, *HDA1*, *HOS1*, *HOS2*, *HOS3*, *HOS4*, *HST1*, *HST2*, *HST3*, and *HST4* are shown in red. (B and D) Ten-fold serial dilutions of the indicated strains carrying either vector alone (pGAL1pr) or a plasmid expressing *HHO1* from a *GAL1* promoter (pGAL1prHHO1) were grown on uracil drop-out media, with either dextrose or galactose as indicated, at 30° for 4 days. (C and E) Immunoblot quantification of Hho1 levels in the indicated strains expressing *HHO1* from a *GAL1* promoter after growth for 20 hr in uracil drop-out media with galactose. Error bars indicate the SE of the mean from three biological replicates.

Histone acetylation negatively regulates linker histone binding in S. cerevisiae

A second class of genes identified in our synthetic dosage screen was those encoding histone deacetylases (HDACs) (Figure 3A), but contrary to mutants with altered histone dosage, mutation of HDACs rescued Hho1 toxicity. To verify that loss of an HDAC could rescue growth of cells with excess Hho1, we created an

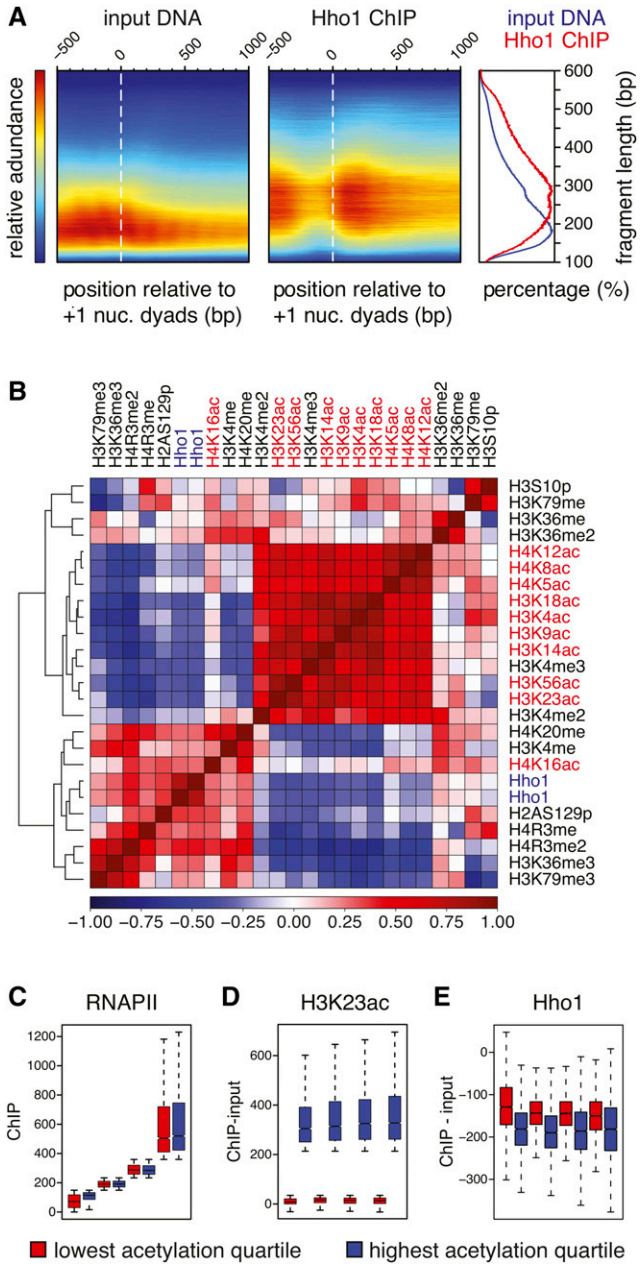

Figure 4 Histone acetylation negatively correlates with linker histone binding in *S. cerevisiae*. (A, left and middle) Two-dimensional occupancy plots of relative sequence fragment abundance, sequence fragment length, and sequence fragment position from input DNA and Hho1 ChIP, relative to the dyad axis of the +1 nucleosomes of 5770 annotated genes in *S. cerevisiae*. Plot was generated using plot2DO (Chereji *et al.* 2017) run with standard settings. The relative sequence read abundance is indicated as a heatmap, the sequence fragment length is plotted on the *y*-axis, and the position of sequence reads relative to the +1 nucleosome is plotted on the *x*-axis. (Right) Plot of sequence fragment lengths from input DNA and Hho1 ChIP-seq of wild-type yeast. (B) Clustered heatmap produced by the deepTools plotCorrelation module (Ramirez *et al.* 2014, 2016). Shown here are the Spearman correlation coefficients of Hho1 occupancy (blue text) at all uniquely mapping yeast nucleosomes (Brogaard *et al.* 2012) with histone post-translational modifications (Weiner *et al.* 2015), including histone acetylation (red text). All data sets were normalized to respective inputs using the Java Genomics Toolkit wigmath.Subtract tool (C–E). All uniquely mapping yeast nucleosomes (Brogaard *et al.* 2012) were binned into quartiles based on RNAPII occupancy (C) and the top and bottom quartiles of H3K23ac (Weiner *et al.* 2015) as calculated using the Java Genomics Toolkit ngs.IntervalStats tool (D). Hho1 occupancy was then plotted for each bin (E). Notches indicate the 95% confidence interval for the median.

*hda1*Δ mutant in our laboratory strain background and confirmed resistance to Hho1 overexpression by dilution plating (Figure 3B). We also confirmed that rescue of growth in an *hda1*Δ mutant was not due to a *GAL1* transcription defect by quantitative immunoblot (Figure 3C). To verify that the impact of HDAC loss is due to loss of deacetylation of core histones, we mutated acetylation sites in the tail of histone H3 to arginine and glutamine to mimic unacetylated and acetylated lysines, respectively. In strains overexpressing Hho1, glutamine substitutions in the H3 tail conferred a growth advantage (Figure 3D), which was not due to altered Hho1 levels (Figure 3E). Collectively, these results suggest that histone acetylation negatively regulates the binding of Hho1 to chromatin.

To further investigate the role of histone acetylation in regulating Hho1 binding, we performed ChIP-seq analysis of Hho1 expressed from its native promoter. To visualize the data generated, we used 2D occupancy plots, which simultaneously display DNA sequencing data as: (1) the relative sequence read abundance (heatmap), (2) sequence fragment length (*y*-axis), and (3) position of sequence reads relative to the dyad of the +1 nucleosome (*x*-axis with the white dashed line indicating the +1 dyad) (Chereji *et al.* 2017). This analysis, presented in Figure 4A, shows that the input DNA used for ChIP was slightly enriched in sequences −400 to +100 bp relative to the +1 nucleosome (left panel), and contained mononucleosome-sized DNA fragments, with the peak of distribution at ∼165 bp (right panel). In contrast, Hho1 antibodies immunoprecipitated primarily larger fragments with a peak of distribution of ∼270 bp (right panel). Interestingly, smaller fragments were present in the Hho1 ChIP, but few small fragments overlapped the +1 nucleosome (middle panel), despite being present in the input (left panel). In contrast, reads overlapping the +1 nucleosome were precipitated with Hho1 if they were longer and also overlapped the +2 nucleosome. Collectively, these data argue that the +1 nucleosome is depleted in Hho1 such that these nucleosomes can only be precipitated with Hho1 antibodies if linked to a +2 nucleosome. This is consistent with previously published work demonstrating that Hho1 fails to cross-link to the 5′ linker of the +1 nucleosome (Rhee *et al.* 2014).

Depletion of Hho1 over the +1 nucleosomes is consistent with the fact that these nucleosomes tend to be highly acetylated. To determine if histone acetylation and Hho1 inversely correlate genome-wide, we quantified the levels of Hho1 and multiple histone post-translational modifications (Weiner *et al.* 2015) over the 67,523 annotated yeast nucleosomes (Brogaard *et al.* 2012) and generated a pairwise Spearman correlation matrix with hierarchical clustering. Figure 4B shows that Hho1 occupancy clustered with histone H4R3 monomethylation and

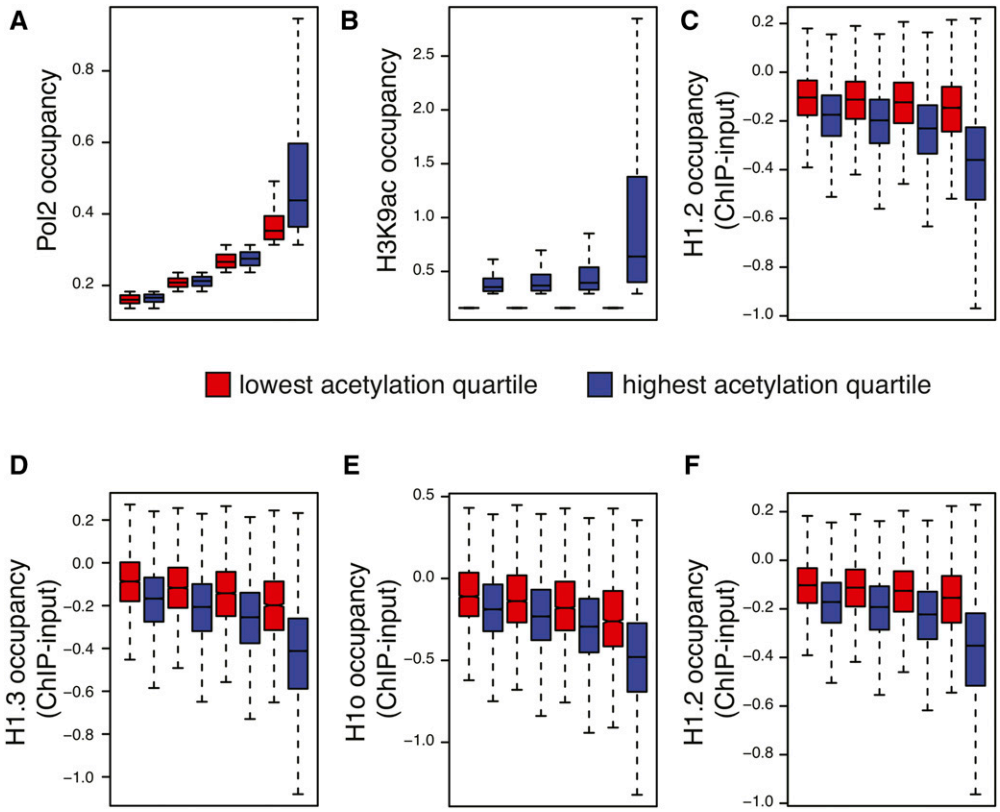

Figure 5 Histone acetylation negatively correlates with linker histone binding in mouse embryonic stem cells. The mouse genome was divided into 1000-bp windows, stepping 500 bp. Windows were divided into four quartiles based on Pol2 (GSM723019) occupancy (A) and the top and bottom quartiles for H3K9ac (GSM1000127) occupancy (B) as determined using the Java Genomics Toolkit ngs.IntervalStats tool. H1.2, H1.3, and H1o occupancies (Cao *et al.* 2013) were then plotted for each bin (C–E, respectively). Notches indicate the 95% confidence interval for the median. (F) Identical analysis as in C, but windows were binned based on H3K27ac (GSM1000099) instead of H3K9ac.

H2AS129 phosphorylation. Little is known about the function of H4R3 methylation in yeast, but H2AS129p is enriched at repressed protein-coding genes (Szilard *et al.* 2010), consistent with a role of Hho1 in negatively regulating transcription. In contrast, except for H4K16ac, all histone acetylation marks in yeast clustered away from Hho1 occupancy with inverse correlation coefficients consistent with the negative regulation of linker histone binding by histone acetylation.

An explanation for the inverse correlation between acetylation and linker histone occupancy observed in Figure 4B is that transcription, which is linked to acetylation, disrupts the interaction of Hho1 with chromatin. Indeed, data supporting this possibility have been published (Schafer *et al.* 2008). To discount a role of transcription in regulating Hho1 binding, we took advantage of the fact that the association between acetylation and transcription is not absolute. For example, while RNAPII traverses the entirety of a gene, histone acetylation is limited to the 5′ end of the transcribed unit. Thus, pools of nucleosomes can be identified that share similar levels of RNAPII but have different amounts of histone acetylation. To determine whether the inverse correlation between Hho1 and histone acetylation is due to the presence of RNAPII, we divided yeast nucleosomes into quartile bins based on RNAPII occupancy as determined in Hobson *et al.* (2012). We further divided each of the resulting bins based on histone acetylation and identified nucleosomes in each bin with high (top quartile, blue) and low (bottom quartile, red) levels of H3K23ac or other acetylation marks (Weiner *et al.* 2015). Figure 4, C and D show the amounts of RNAPII and H3K23ac in the eight resulting bins, respectively. We then calculated Hho1 occupancy for each bin and plotted it as a box plot (Figure 4E for H3K23ac and Figure S2 in File S1 for other acetylation sites). The results show that nucleosomes with increased H3K23ac had reduced Hho1 occupancy when levels of RNAPII were normalized, indicating that differing RNAPII levels were not responsible for altered Hho1 occupancy. Similar trends were observed when analyzing other acetylation marks (Figure S2 in File S1). Additionally, comparable results were obtained when analyzing linker histone H1.2, H1.3, and H1o occupancy (Cao *et al.* 2013) in mouse embryonic stem cells relative to H3K9ac (Figure 5, A–E) and H3K27ac (Figure 5F). Collectively, these results suggest that acetylated chromatin is refractory to linker histone binding in *S. cerevisiae* and other organisms.

Discussion

In this study, we investigated the regulation of linker histone binding in the yeast, *S. cerevisiae*. A major factor thought to regulate linker histone levels in chromatin is the abundance of linker histone in the cell. While vertebrate cells contain approximately one linker histone for every nucleosome, *S. cerevisiae* exhibits reduced linker histone levels; albeit the reported stoichiometry relative to nucleosomes varies depending on the study (Woodcock *et al.* 2006). Using a novel approach, we determined that yeast have one molecule of Hho1 for

every ~19 nucleosomes. Previous work using various approaches have estimated the stoichiometry of Hho1 to nucleosomes to be 1:4, 1:10, 1:26, and 1:37 (Freidkin and Katcoff 2001; Downs *et al.* 2003; Ghaemmaghami *et al.* 2003; Kulak *et al.* 2014). Interestingly, the 1:26 ratio, which is the closest to our result, is the only previous study to quantify levels of untagged Hho1 (Kulak *et al.* 2014). Regardless of the exact ratio, all studies agree that Hho1 levels are well below that of nucleosomes, and because linker histones bind and compact chromatin cooperatively (Routh *et al.* 2008), this may be important to prevent formation of higher order chromatin structures on the gene-rich yeast genome.

Consistent with the importance of substoichiometric linker histone levels in *S. cerevisiae*, increased expression resulted in a severe growth defect. Interestingly, this defect was accompanied by only modest increases in linker histone levels at most loci tested. This result was initially surprising since in fibroblasts, overexpressed linker histones can bind chromatin, increasing the overall nucleosome repeat length (Gunjan *et al.* 1999). While we cannot exclude the fact that some of the overexpressed Hho1 is cytoplasmic, and thus not available for chromatin binding, multiple lines of evidence support the hypothesis that short linker DNA in yeast chromatin excludes Hho1. First, previous work shows that Hho1 is enriched in regions with increased spacing between nucleosomes (Ocampo *et al.* 2016), suggesting that linker DNA availability as opposed to linker histone abundance, dictates Hho1 binding. Second, in stationary phase, genic nucleosomes increase their spacing (Zhang *et al.* 2011), which coincides with increased linker histone binding to chromatin (Schafer *et al.* 2008). Finally, chromatin reconstituted on DNA that positions nucleosomes with short linkers is resistant to linker histone binding and compaction (Routh *et al.* 2008). Collectively, these data suggest that histone stoichiometry does not dictate linker histone binding in yeast and instead overexpressed Hho1 likely localizes to limited regions with longer linker DNA, such as the 5′ ends of genes, where it interferes with early stages of transcription.

The preference of Hho1 for binding regions with longer linker DNA, makes the +1 nucleosome, which is adjacent to a nucleosome-depleted region, a seemingly ideal ligand for binding by this linker histone. However, our data, and that of others, show Hho1 depletion from the +1 nucleosome. The molecular basis for this observation was revealed in this study using both genetic and genome-wide approaches, demonstrating that histone tail acetylation negatively regulates Hho1 binding. Since the 5′ ends of transcribed genes are highly acetylated, these regions may be largely refractory to Hho1 binding. The ability of histone acetylation to hamper the binding of Hho1 is not surprising, as others have observed increased linker histone mobility in cells treated with HDAC inhibitors (Raghuram *et al.* 2010). Together our data support a model in which histone acetylation, not histone stoichiometry, plays a dominant role in regulating linker histone binding in *S. cerevisiae*. Moreover, our results shed light on the puzzling finding that despite their role in compacting chromatin, depletion of linker histones does not result in global upregulation of gene expression (Shen and Gorovsky 1996; Freidkin and Katcoff 2001; Fan *et al.* 2005). Since acetylation likely excludes linker histones from regions of transcriptional activity, their depletion has little impact on steady-state transcription. Future work in our laboratory will focus on the impact that Hho1 has on transcriptional reprogramming in *S. cerevisiae*.

Acknowledgments

We gratefully acknowledge Apryl Northrup for generation of plasmids and Fred Winston for providing yeast strains and plasmids. This work was supported by a Discovery Grant awarded to L.J.H. from the Natural Sciences and Engineering Research Council of Canada (NSERC). B.J.E.M. and J.K.C. were recipients of NSERC Canada Graduate Scholarship awards and N.A.T.I. was supported by an NSERC Undergraduate Student Research Award.

Literature Cited

Bednar, J., I. Garcia-Saez, R. Boopathi, A. R. Cutter, G. Papai *et al.*, 2017 Structure and dynamics of a 197 bp nucleosome in complex with linker histone H1. Mol. Cell 66: 384–397.e8.

Bernier, M., Y. Luo, K. C. Nwokelo, M. Goodwin, S. J. Dreher *et al.*, 2015 Linker histone H1 and H3K56 acetylation are antagonistic regulators of nucleosome dynamics. Nat. Commun. 6: 10152.

Brogaard, K., L. Xi, J. P. Wang, and J. Widom, 2012 A map of nucleosome positions in yeast at base-pair resolution. Nature 486: 496–501.

Bustin, M., F. Catez, and J. H. Lim, 2005 The dynamics of histone H1 function in chromatin. Mol. Cell 17: 617–620.

Cao, K., N. Lailler, Y. Zhang, A. Kumar, K. Uppal *et al.*, 2013 High-resolution mapping of h1 linker histone variants in embryonic stem cells. PLoS Genet. 9: e1003417.

Chereji, R. V., J. Ocampo, and D. J. Clark, 2017 MNase-sensitive complexes in yeast: nucleosomes and non-histone barriers. Mol. Cell 65: 565–577.e3.

Chruscicki, A., V. E. Macdonald, B. P. Young, C. J. Loewen, and L. J. Howe, 2010 Critical determinants for chromatin binding by Saccharomyces cerevisiae Yng1 exist outside of the plant homeodomain finger. Genetics 185: 469–477.

Downs, J. A., E. Kosmidou, A. Morgan, and S. P. Jackson, 2003 Suppression of homologous recombination by the Saccharomyces cerevisiae linker histone. Mol. Cell 11: 1685–1692.

Duina, A. A., and F. Winston, 2004 Analysis of a mutant histone H3 that perturbs the association of Swi/Snf with chromatin. Mol. Cell. Biol. 24: 561–572.

Fan, Y., T. Nikitina, J. Zhao, T. J. Fleury, R. Bhattacharyya *et al.*, 2005 Histone H1 depletion in mammals alters global chromatin structure but causes specific changes in gene regulation. Cell 123: 1199–1212.

Freidkin, I., and D. J. Katcoff, 2001 Specific distribution of the Saccharomyces cerevisiae linker histone homolog HHO1p in the chromatin. Nucleic Acids Res. 29: 4043–4051.

Ghaemmaghami, S., W. K. Huh, K. Bower, R. W. Howson, A. Belle *et al.*, 2003 Global analysis of protein expression in yeast. Nature 425: 737–741.

Gunjan, A., B. T. Alexander, D. B. Sittman, and D. T. Brown, 1999 Effects of H1 histone variant overexpression on chromatin structure. J. Biol. Chem. 274: 37950–37956.

Happel, N., and D. Doenecke, 2009 Histone H1 and its isoforms: contribution to chromatin structure and function. Gene 431: 1–12.
Hobson, D. J., W. Wei, L. M. Steinmetz, and J. Q. Svejstrup, 2012 RNA polymerase II collision interrupts convergent transcription. Mol. Cell 48: 365–374.
Ikebe, J., S. Sakuraba, and H. Kono, 2016 H3 histone tail conformation within the nucleosome and the impact of K14 acetylation studied using enhanced sampling simulation. PLoS Comput. Biol. 12: e1004788.
Izzo, A., K. Kamieniarz-Gdula, F. Ramirez, N. Noureen, J. Kind *et al.*, 2013 The genomic landscape of the somatic linker histone subtypes H1.1 to H1.5 in human cells. Cell Rep. 3: 2142–2154.
Kim, J., J. Lee, and T. H. Lee, 2015 Lysine acetylation facilitates spontaneous DNA dynamics in the nucleosome. J. Phys. Chem. B 119: 15001–15005.
Kulak, N. A., G. Pichler, I. Paron, N. Nagaraj, and M. Mann, 2014 Minimal, encapsulated proteomic-sample processing applied to copy-number estimation in eukaryotic cells. Nat. Methods 11: 319–324.
Kurat, C. F., J. Recht, E. Radovani, T. Durbic, B. Andrews *et al.*, 2014 Regulation of histone gene transcription in yeast. Cell. Mol. Life Sci. 71: 599–613.
Kushnirov, V. V., 2000 Rapid and reliable protein extraction from yeast. Yeast 16: 857–860.
Li, H., and R. Durbin, 2010 Fast and accurate long-read alignment with Burrows-Wheeler transform. Bioinformatics 26: 589–595.
Luger, K., A. W. Mader, R. K. Richmond, D. F. Sargent, and T. J. Richmond, 1997 Crystal structure of the nucleosome core particle at 2.8 A resolution. Nature 389: 251–260.
Maltby, V. E., B. J. Martin, J. M. Schulze, I. Johnson, T. Hentrich *et al.*, 2012a Histone H3 lysine 36 methylation targets the Isw1b remodeling complex to chromatin. Mol. Cell. Biol. 32: 3479–3485.
Maltby, V. E., B. J. E. Martin, J. Brind'Amour, A. T. Chruscicki, K. L. McBurney *et al.*, 2012b Histone H3K4 demethylation is negatively regulated by histone H3 acetylation in Saccharomyces cerevisiae. Proc. Natl. Acad. Sci. USA 109: 18505–18510.
Martin, B. J., K. L. McBurney, V. E. Maltby, K. N. Jensen, J. Brind'Amour *et al.*, 2017 Histone H3K4 and H3K36 methylation independently recruit the NuA3 histone acetyltransferase in Saccharomyces cerevisiae. Genetics 205: 1113–1123.
Meyer, S., N. B. Becker, S. H. Syed, D. Goutte-Gattat, M. S. Shukla *et al.*, 2011 From crystal and NMR structures, footprints and cryo-electron-micrographs to large and soft structures: nanoscale modeling of the nucleosomal stem. Nucleic Acids Res. 39: 9139–9154.
Millan-Arino, L., A. B. Islam, A. Izquierdo-Bouldstridge, R. Mayor, J. M. Terme *et al.*, 2014 Mapping of six somatic linker histone H1 variants in human breast cancer cells uncovers specific features of H1.2. Nucleic Acids Res. 42: 4474–4493.
Mumberg, D., R. Muller, and M. Funk, 1994 Regulatable promoters of Saccharomyces cerevisiae: comparison of transcriptional activity and their use for heterologous expression. Nucleic Acids Res. 22: 5767–5768.
Neumann, H., S. M. Hancock, R. Buning, A. Routh, L. Chapman *et al.*, 2009 A method for genetically installing site-specific acetylation in recombinant histones defines the effects of H3 K56 acetylation. Mol. Cell 36: 153–163.
Ocampo, J., R. V. Chereji, P. R. Eriksson, and D. J. Clark, 2016 The ISW1 and CHD1 ATP-dependent chromatin remodelers compete to set nucleosome spacing in vivo. Nucleic Acids Res. 44: 4625–4635.
Raghuram, N., G. Carrero, T. J. Stasevich, J. G. McNally, J. Th'ng *et al.*, 2010 Core histone hyperacetylation impacts cooperative behavior and high-affinity binding of histone H1 to chromatin. Biochemistry 49: 4420–4431.
Ramirez, F., F. Dundar, S. Diehl, B. A. Gruning, and T. Manke, 2014 DeepTools: a flexible platform for exploring deep-sequencing data. Nucleic Acids Res. 42: W187–W191.
Ramirez, F., D. P. Ryan, B. Gruning, V. Bhardwaj, F. Kilpert *et al.*, 2016 DeepTools2: a next generation web server for deep-sequencing data analysis. Nucleic Acids Res. 44: W160–W165.
Rhee, H. S., A. R. Bataille, L. Zhang, and B. F. Pugh, 2014 Subnucleosomal structures and nucleosome asymmetry across a genome. Cell 159: 1377–1388.
Routh, A., S. Sandin, and D. Rhodes, 2008 Nucleosome repeat length and linker histone stoichiometry determine chromatin fiber structure. Proc. Natl. Acad. Sci. USA 105: 8872–8877.
Schafer, G., C. R. McEvoy, and H. G. Patterton, 2008 The Saccharomyces cerevisiae linker histone Hho1p is essential for chromatin compaction in stationary phase and is displaced by transcription. Proc. Natl. Acad. Sci. USA 105: 14838–14843.
Shen, X., and M. A. Gorovsky, 1996 Linker histone H1 regulates specific gene expression but not global transcription in vivo. Cell 86: 475–483.
Simon, M., J. A. North, J. C. Shimko, R. A. Forties, M. B. Ferdinand *et al.*, 2011 Histone fold modifications control nucleosome unwrapping and disassembly. Proc. Natl. Acad. Sci. USA 108: 12711–12716.
Syed, S. H., D. Goutte-Gattat, N. Becker, S. Meyer, M. S. Shukla *et al.*, 2010 Single-base resolution mapping of H1-nucleosome interactions and 3D organization of the nucleosome. Proc. Natl. Acad. Sci. USA 107: 9620–9625.
Szilard, R. K., P. E. Jacques, L. Laramee, B. Cheng, S. Galicia *et al.*, 2010 Systematic identification of fragile sites via genome-wide location analysis of gamma-H2AX. Nat. Struct. Mol. Biol. 17: 299–305.
van Bakel, H., K. Tsui, M. Gebbia, S. Mnaimneh, T. R. Hughes *et al.*, 2013 A compendium of nucleosome and transcript profiles reveals determinants of chromatin architecture and transcription. PLoS Genet. 9: e1003479.
Van Holde, K. E., 1989 *Chromatin*. Springer-Verlag, New York.
Weiner, A., H. V. Chen, C. L. Liu, A. Rahat, A. Klien *et al.*, 2012 Systematic dissection of roles for chromatin regulators in a yeast stress response. PLoS Biol. 10: e1001369.
Weiner, A., T. H. Hsieh, A. Appleboim, H. V. Chen, A. Rahat *et al.*, 2015 High-resolution chromatin dynamics during a yeast stress response. Mol. Cell 58: 371–386.
Woodcock, C. L., A. I. Skoultchi, and Y. Fan, 2006 Role of linker histone in chromatin structure and function: H1 stoichiometry and nucleosome repeat length. Chromosome Res. 14: 17–25.
Young, B. P., and C. J. Loewen, 2013 Balony: a software package for analysis of data generated by synthetic genetic array experiments. BMC Bioinformatics 14: 354.
Zhang, L., H. Ma, and B. F. Pugh, 2011 Stable and dynamic nucleosome states during a meiotic developmental process. Genome Res. 21: 875–884.
Zhou, B. R., H. Feng, H. Kato, L. Dai, Y. Yang *et al.*, 2013 Structural insights into the histone H1-nucleosome complex. Proc. Natl. Acad. Sci. USA 110: 19390–19395.
Zhou, B. R., J. Jiang, H. Feng, R. Ghirlando, T. S. Xiao *et al.*, 2015 Structural mechanisms of nucleosome recognition by linker histones. Mol. Cell 59: 628–638.

Communicating editor: O. Rando